Human Molecular Genetics, 2004, Vol. 13, No. 20 **2505–2518**
doi:10.1093/hmg/ddh266
Advance Access published on August 18, 2004

Transgenic overexpression of human *DMPK* accumulates into hypertrophic cardiomyopathy, myotonic myopathy and hypotension traits of myotonic dystrophy

D. Fearghas O'Cochlain[1,2], Carmen Perez-Terzic[1,2,3], Santiago Reyes[1,2], Garvan C. Kane[1,2], Atta Behfar[1,2], Denice M. Hodgson[1,2], Jeffrey A. Strommen[3], Xiao-Ke Liu[1,2], Walther van den Broek[4], Derick G. Wansink[4], Bé Wieringa[4] and Andre Terzic[1,2,*]

[1]Division of Cardiovascular Diseases, Department of Medicine, [2]Department of Molecular Pharmacology and Experimental Therapeutics and [3]Department of Physical Medicine and Rehabilitation, Mayo Clinic College of Medicine, Rochester, MN, USA and [4]Department of Cell Biology, Nijmegen Center for Molecular Life Sciences, University Medical Center, Nijmegen, The Netherlands

Received July 2, 2004; Revised July 26, 2004; Accepted August 4, 2004

Abnormal expression of human myotonic dystrophy protein kinase (*hDMPK*) gene products has been implicated in myotonic dystrophy type 1 (DM1), yet the impact of distress accumulation produced by persistent overexpression of this poorly understood member of the Rho kinase-related protein kinase gene-family remains unknown. Here, in the aged transgenic murine line carrying approximately 25 extra copies of a complete *hDMPK* gene with all exons and an intact promoter region (Tg26-hDMPK), overexpression of mRNA and protein transgene products in cardiac, skeletal and smooth muscles resulted in deficient exercise endurance, an integrative index of muscle systems underperformance. In contrast to age-matched (11–15 months) wild-type controls, hearts from Tg26-hDMPK developed cardiomyopathic remodeling with myocardial hypertrophy, myocyte disarray and interstitial fibrosis. Hypertrophic cardiomyopathy was associated with a propensity for dysrhythmia and characterized by overt intracellular calcium overload promoting nuclear translocation of transcription factors responsible for maladaptive gene reprograming. Skeletal muscles in distal limbs of Tg26-hDMPK showed myopathy with myotonic discharges coupled with deficit in sarcolemmal chloride channels, required regulators of hyperexcitability. Fiber degeneration in Tg26-hDMPK resulted in sarcomeric disorganization, centralization of nuclei and tubular aggregation. Moreover, the reduced blood pressure in Tg26-hDMPK indicated deficient arterial smooth muscle tone. Thus, the cumulative stress induced by permanent overexpression of *hDMPK* gene products translates into an increased risk for workload intolerance, hypertrophic cardiomyopathy with dysrhythmia, myotonic myopathy and hypotension, all distinctive muscle traits of DM1. Proper expression of *hDMPK* is, therefore, mandatory in supporting the integral balance among cytoarchitectural infrastructure, ion-homeostasis and viability control in various muscle cell types.

INTRODUCTION

Myotonic dystrophy protein kinase (DMPK), first cloned and identified as a protein kinase more than a decade ago, is a member of the AGC family of serine–threonine kinases (1,2). While significant progress has been made in deciphering the role of homologous kinases like myotonic dystrophy kinase-related Cdc42-binding kinase, Rho kinases ROCK-I/II

*To whom correspondence should be addressed at: Department of Medicine and Department of Molecular Pharmacology and Experimental Therapeutics, Guggenheim 7, Mayo Clinic, 200 First Street SW, Rochester, MN 55905, USA. Tel: +1 5072847517; Fax: +1 5072849111; Email: terzic.andre@mayo.edu

and citron kinase, which modulate the actin cytoskeleton and are implicated in stress fiber formation, cell motility and cytokinesis (3), the physiological contribution of DMPK has remained rather elusive.

Molecular assays have recently revealed that DMPK may interact with a variety of cellular substrates, including phospholemman, the dihydropyridine receptor, the CUG binding protein CUGBP/hNab50 and the myosin phosphatase targeting subunit 1 (4,5). Yet, the relevance of these *in vitro* findings for the *in vivo* specificity of DMPK is still uncertain (6). Moreover, DMPK transcripts undergo alternative splicing, which is regulated in a cell-type dependent manner and leads to the production of distinct protein isoforms partitioned between the cytosol, mitochondria and endoplasmic reticulum (5–8). In this way, DMPK has been implicated in diverse cellular functions, ranging from modulation of the contraction–relaxation cycle and ion handling to cytoskeletal movement and organelle localization in various muscle tissue types, where DMPK is primarily expressed (9–20).

Expansion of the unstable $(CTG)_n$ repeat within the 3′-untranslated region (3′-UTR) of the human *DMPK* (*hDMPK*), encoded at chromosome region 19q13.3, causes myotonic dystrophy type 1 (DM1), an autosomal dominant disease with multisystemic phenotype (21–24). Although DM1 is pleiotropic with a range of systemic abnormalities, the predilection of *hDMPK* expression for muscle tissues is reflected in typical features of myotonic dystrophy that include muscle weakness and myotonic skeletal myopathy, cardiomyopathy with cardiac conduction disturbances and smooth muscle manifestations (2). The pathobiological significance and fate of the primary product of *hDMPK*, i.e. DMPK (pre)mRNA with long expanded $(CUG)_n$ repeats from the mutant DMPK allele, have been associated with inhibition of myogenesis (25–28). A toxic RNA-gain-of-function is proposed to form ribonuclear inclusions by sequestering essential RNA splicing and transcription factors bound to the expanded $(CUG)_n$ repeat in the DMPK-(pre)mRNA 3′-UTR, thereby interfering with cell development or viability control (29–31). Importantly, the severity of the disease correlates with the size of repeat expansion, and symptoms worsen with age (2). Although abnormal expression of *hDMPK* products is implicated in DM1, the impact of distress accumulation produced by persistent overexpression of this serine–threonine protein kinase gene-family member remains unknown.

Therefore, a transgenic murine line, named Tg26-hDMPK, carrying approximately 25 extra copies of the fully intact *hDMPK* bearing a $(CTG)_{11}$ repeat tract with normal tissue distribution was maintained over multiple generations. Whereas the young Tg26-hDMPK displayed mild myopathic symptoms (9), the present characterization of the older (11–15 months) phenotype revealed that age-associated stress accumulation triggers multisystemic derangements with cardiovascular compromise, skeletal and smooth muscle abnormalities, recapitulating diverse muscle traits of myotonic dystrophy. These consequences of overproduction of wild-type (WT) hDMPK protein and/or mRNA were coupled to cytoarchitectural derangements and distortion of ionic homeostasis in heart, skeletal muscle and smooth muscle cells. Thus, the Tg26-hDMPK overexpressor murine line proves to be a valuable model in evaluating the effects of augmented doses of $(CUG)_n$ repeats in the DMPK mRNA pool and prolonged over-activity of protein products from the *DMPK* gene.

RESULTS

Transgenic overexpression of *hDMPK* reduces workload tolerance

From a series of transgenic mice that tandemly integrate copies of a 14 kb genomic *Nhe*I fragment, which spans the entire human *DMPK* (*hDMPK*) gene and includes the full intergenic region up to the 3′ end of the *DMWD* (*Dmrn9*) gene upstream of *DMPK*, *hDMPK* overexpressors were selected to carry multiple copies of the intact *hDMPK* gene with a normal size $(CTG)_{11}$ repeat (9; Fig. 1A). The transgene contains most, if not all, regulatory elements that drive proper expression of *DMPK* gene products (9,32), and initial typing at young age (up to 8–10 weeks old) revealed that mice with high copy numbers of *hDMPK* genes exhibit breeding difficulty and mild cardiac hypertrophy, independent of the transgene integration site. The severity of the presentation appeared transgene-copy number dependent (9). To rule out intergenerational differences that could relate to epigenetic modification or instability of the transgene cluster possibly influencing phenotypic manifestation, animals with approximately 25 *hDMPK* copies, i.e. the Tg26-hDMPK line, were further maintained for over 20 generations. Northern (Fig. 1B) and western blot analyses (Fig. 1C) of the Tg26-hDMPK indicated significant overexpression of both DMPK mRNA and protein in cardiac and skeletal muscles, as well as in smooth muscle-containing organs. This is in accord with the natural predilection of DMPK for muscle tissues, and corresponds to tissue distribution of DMPK mRNA and protein in both human and mouse samples (8,33). Phosphoimage quantification of northern blots revealed *DMPK* mRNA levels 15.1-, 2.9- and 2.0-fold higher in Tg26-hDMPK compared with the endogenous *DMPK* mRNA in heart, skeletal muscle and smooth muscle of WT (FVB background) controls (Fig. 1B). Accordingly, densitometric quantitation of western blot signals demonstrated a 7.5-, 2.0- and 5.2-fold higher DMPK protein expression in Tg26-hDMPK compared with intrinsic DMPK protein in WT heart, skeletal muscle and smooth muscle, respectively (Fig. 1C). Furthermore, the isoform distribution in Tg26-hDMPK, with long DMPK variants predominant in heart and skeletal muscle and short variants predominant in smooth muscle, was in line with the established tissue distribution of alternative splice variants (Fig. 1D; 7). Thus, the selected Tg26-hDMPK line is a genuine model to probe the long-term cumulative effects of overproduction of *hDMPK* gene products in the three distinct muscle types in the body.

The integrative function of muscle systems is reflected by the tolerance to imposed exertion, an indicator of overall physical endurance (34). Under exercise stress testing, 11 to 15-month-old Tg26-hDMPK mice performed at a significantly reduced level compared with age-matched WT controls (Fig. 2A). The tolerated workload, a parameter that incorporates time of effort with speed and incline of the treadmill regimen, was 3-fold lower in Tg26-hDMPK ($n = 10$)

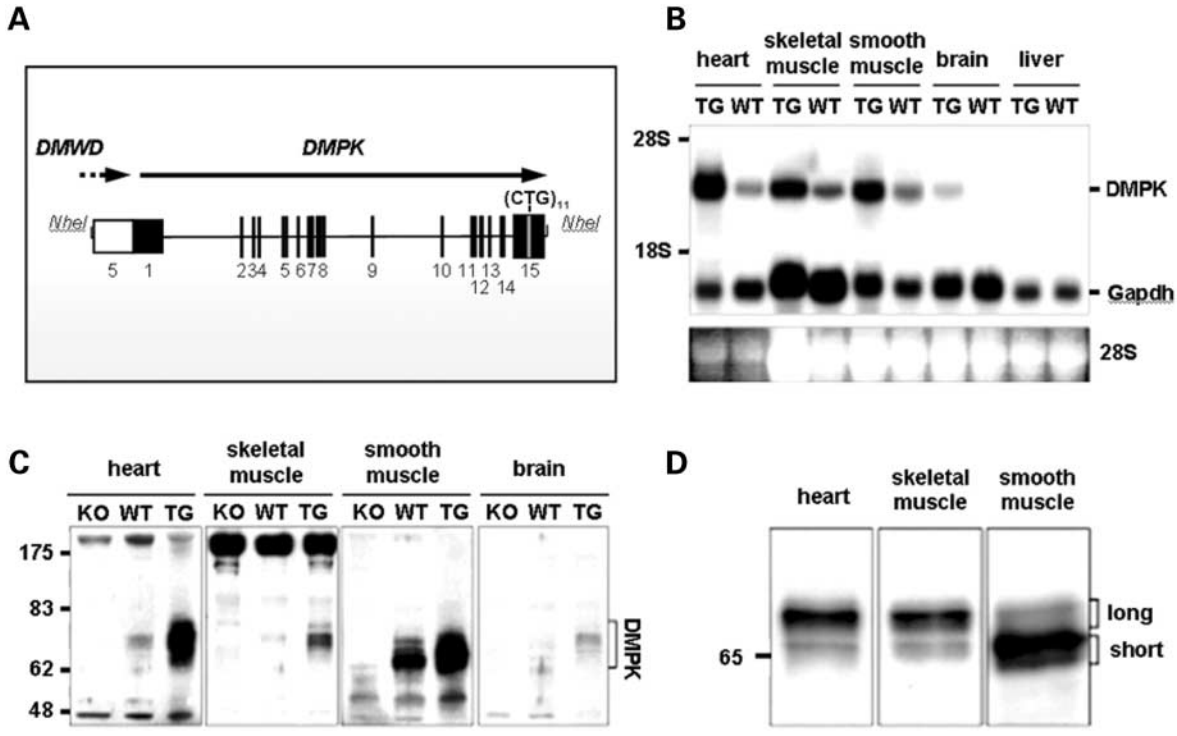

Figure 1. Overexpression of the *hDMPK* transgene. (**A**) The human *DMPK* transgene construct, an ~14 kb genomic *Nhe* I fragment containing all the 15 *DMPK* exons (black boxes) and the last *DMWD* exon (white box), including essential *DMPK* promoter sequences, used to generate the Tg26-hDMPK (TG) mice. Exons are numbered, and the transcriptional orientation of *DMPK* and *DMWD* are indicated with arrows. Location of the $(CTG)_{11}$ repeat is highlighted in dark grey within exon 15. (**B**) Northern blot analysis of TG versus WT mice demonstrates a 15.1-, 2.9-, 2.0-, 8.4- and 1.4-fold increase in *DMPK* mRNA expression in heart, skeletal muscle, smooth muscle, brain and liver, respectively, as determined by phosphoimage analysis using tissue-specific Gapdh signals for normalization. Corresponding 28S rRNA signals are shown below. (**C**) Western blot analysis, using the B79 DMPK antibody, demonstrates a 7.5-, 2.0-, 5.2- and 1.5-fold increase in DMPK protein expression in heart, skeletal muscle, smooth muscle and brain, respectively in TG versus WT determined by densitometry. Molecular weight markers are indicated in kiloDaltons DMPK isoform-specific signals are observed within the ~65–75 kDa range; and as a control for non-specific antibody binding, specimens from DMPK-null (KO) mice are presented. (**D**) High resolution western blotting of tissue-specific DMPK isoform expression profiles in TG heart, skeletal muscle and smooth muscle. Long human DMPK isoforms are mainly expressed in heart and skeletal muscle, whereas short isoforms predominate in smooth muscle.

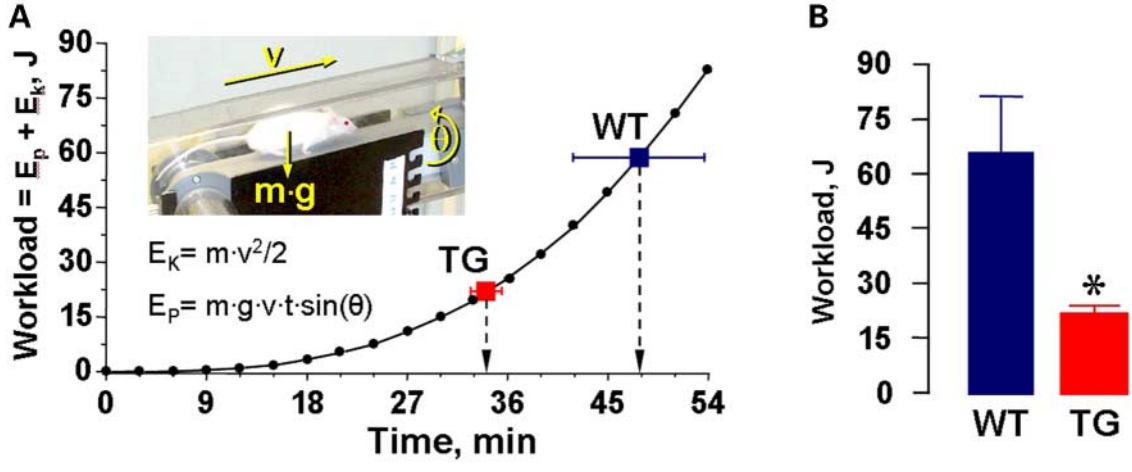

Figure 2. *hDMPK* overexpression translates into exertional intolerance. (**A** and **B**) Exercise stress testing, with a graded treadmill protocol, revealed a significant performance disadvantage in Tg26-hDMPK (TG) compared with WT mice. Workload was defined as a sum of kinetic E_k and potential E_p energy of the treadmill-exercised mice, where m represents animal mass, v running velocity, g acceleration due to gravity, t elapsed time at a protocol level and θ angle of incline. Time of drop-out (indicated by arrowheads in A) was defined by failure to sustain performance at a given workload level (plotted in B). *, $P < 0.05$.

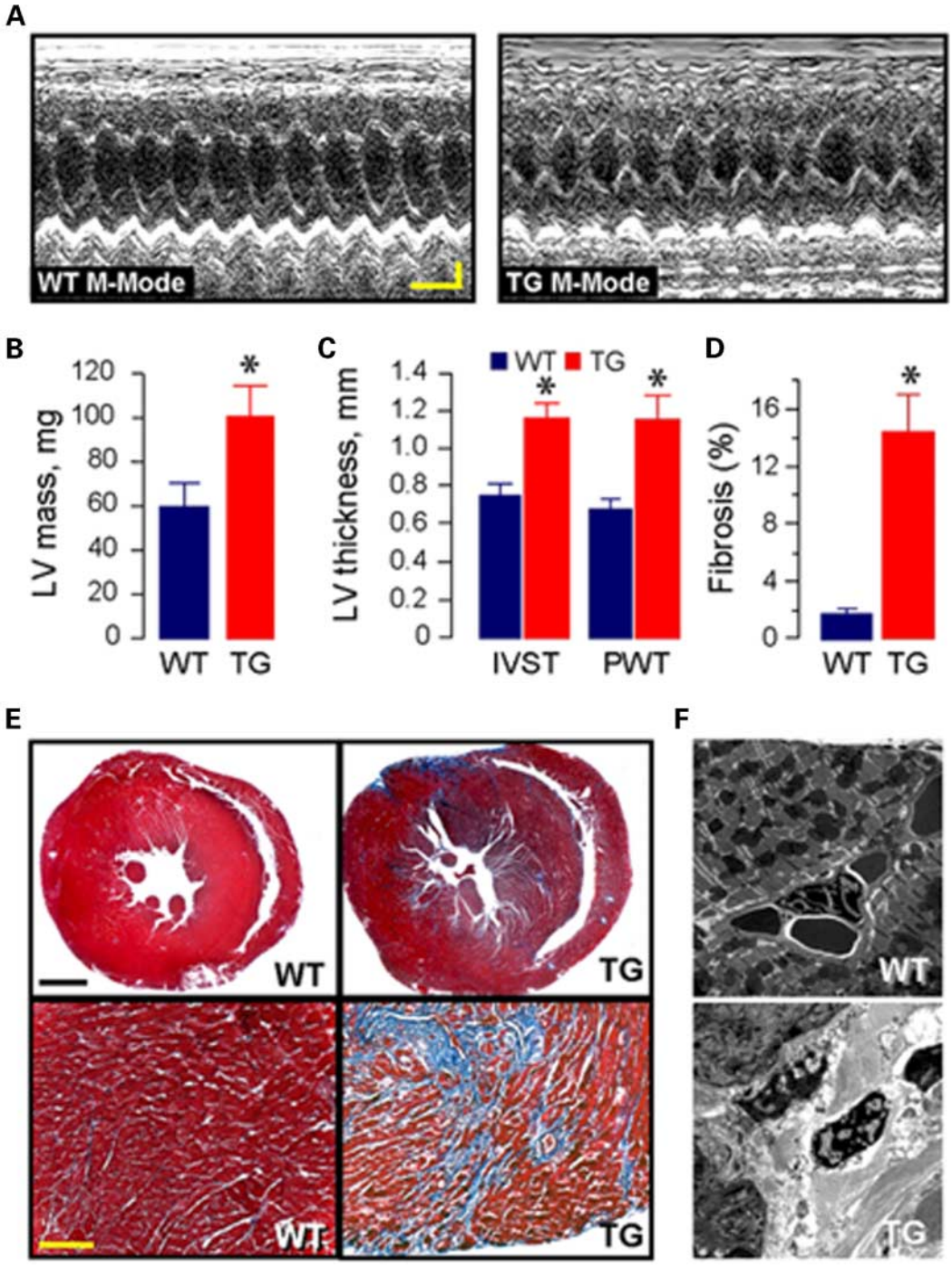

Figure 3. Hypertrophic cardiac remodeling with fibrosis in the *hDMPK* overexpressor. (**A**) M-mode echocardiography (vertical bar: 1 mm, horizontal bar: 100 ms) shows LV hypertrophy in Tg26-hDMPK (TG; right), compared with WT (left), with significant increase in LV mass (**B**), interventricular septal thickness (IVST; **C**) and posterior wall thickness (PWT; C). Masson's trichrome staining reveals massive cardiac interstitial fibrosis in TG compared with WT presented as average values (**D**) or as individual histological specimens (**E**) at 6.3×(upper, bar: 1 mm) and 20×(lower, bar: 500 μm) magnifications. (**F**) Ultrastructural evaluation by transmission electron microscopy further demonstrates extensive fibrosis in TG compared with WT. *, $P < 0.05$ in B–D.

compared with WT ($n = 10$), indicating impaired bodily response to physical challenge ($P < 0.05$; Fig. 2B). Thus, overexpression of *hDMPK* produces an abnormal phenotype characterized by poor workload tolerance indicating compromised muscle systems.

Hypertrophic cardiomyopathic remodeling in the *hDMPK* overexpressor

Maladaptive structural remodeling indicates profound intolerance of heart muscle to stress (35). While mild cardiac

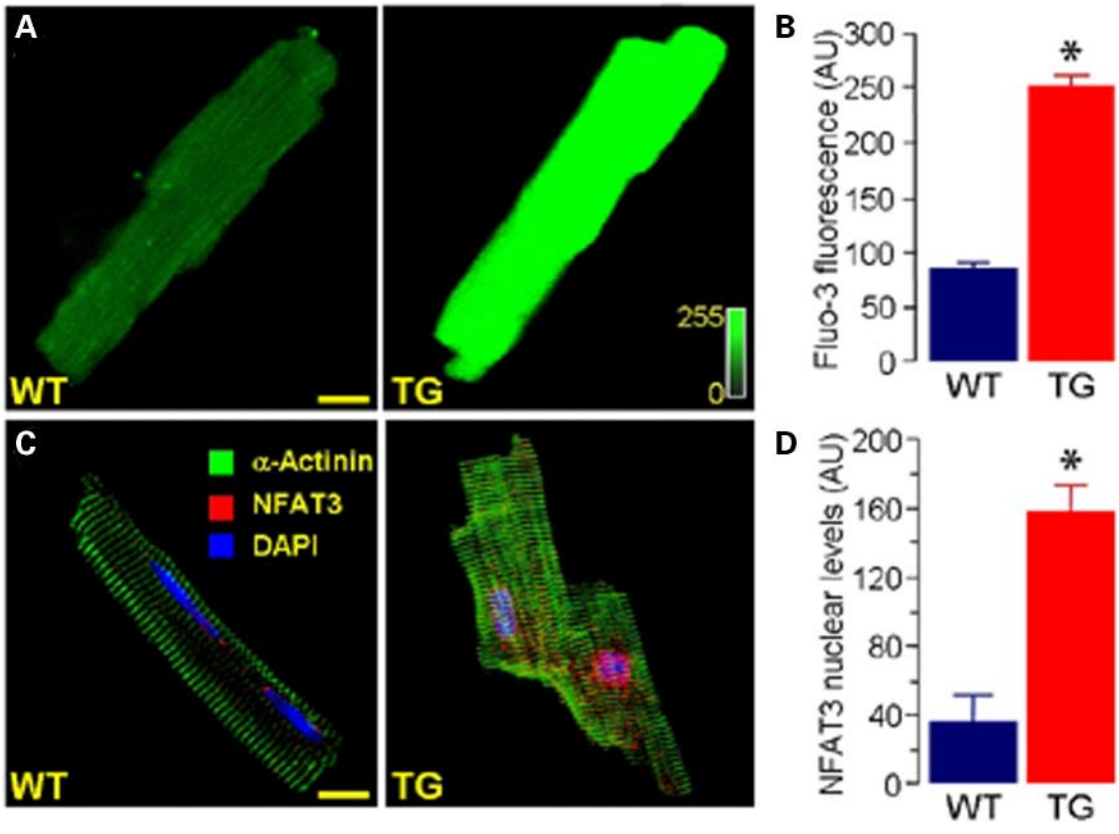

Figure 4. Calcium overload and nuclear overexpression of cardiac transcription regulators in Tg26-hDMPK (TG) cardiomyocytes. (**A** and **B**) Isolated TG, but not WT, cardiac cells loaded with the Ca^{2+}-sensitive indicator Fluo3-AM demonstrate, on laser confocal microscopy, intracellular calcium overload. (**C** and **D**) Compared with immunostained WT, isolated cardiomyocytes of TG, stained with the cardiac sarcomeric marker α-actinin, present increased expression of the nuclear factor of activated T cells NFAT3, a prototypic transcription regulator of pathologic cardiac hypertrophy, with evidence of nuclear localization confirmed by co-localization with the nuclear marker DAPI. Bars, 20 μm. Average values presented in arbitrary units (AU). *, $P < 0.05$.

remodeling was observed in younger mice overexpressing *hDMPK* (9), M-mode echocardiography, performed here under light isoflurane anesthesia, captured significant ventricular hypertrophy in hearts from old (11–15 months) Tg26-hDMPK mice that was not observed in age-matched WT controls (Fig. 3A). On average ($n = 6$ in each group), the calculated left ventricular (LV) mass was essentially doubled from 59 ± 10 mg in WT to 100 ± 14 mg in Tg26-hDMPK ($P < 0.04$; Fig. 3B). Interventricular septal thickness (1.16 ± 0.08 mm versus 0.75 ± 0.06 mm; $P < 0.0001$) and posterior wall thickness (1.15 ± 0.13 mm versus 0.68 ± 0.04 mm; $P < 0.001$) were both significantly greater in Tg26-hDMPK than WT hearts (Fig. 3C). Moreover, Masson's trichrome stain, used to differentiate collagen from cardiomyocytes, showed a marked increase in cardiac interstitial fibrosis in Tg26-hDMPK hearts (Fig. 3D and E). On quantification ($n = 5$ in each group), a 7-fold increase in fibrosis was detectable in Tg26-hDMPK compared with WT, i.e. 14 ± 3% versus 2 ± 1%, respectively ($P < 0.002$; Fig. 3D), further highlighted at the ultrastructural level by electron microscopy (Fig. 3F). Hence, *hDMPK* overexpression triggers structural myocardial maladaptation with age-accumulated stress.

Pathologic hypertrophic remodeling is typically initiated by calcium mishandling that induces gene reprograming (36). Here, intracellular calcium overload (Fig. 4A and B) and nuclear translocation of the prototypic calcium-dependent cardiac transcription factor NFAT3, the nuclear factor of activated T cells (Fig. 4C and D), an established effector of growth signaling (36,37), were both prominent in Tg26-hDMPK but absent from WT. Ultrastructural imaging, by field emission scanning electron microscopy, revealed in Tg26-hDMPK but not WT pronounced myocyte disarray (Fig. 5A and B), with subcellular degenerative changes, including nuclear deformity, multiple vacuolization and mitochondria with abnormal cristae on transmission electron microscopy (Fig. 5C–F). Collectively, these abnormalities in cellular architecture are a pathological hallmark of cardiomyopathy.

Structural deficits were associated with electrical disturbances manifested as ventricular tachyarrhythmias captured on telemetry in the ambulatory Tg26-hDMPK, but absent from the WT (Fig. 6A and B). Under light sedation, numerous additional electrocardiographic (ECG) abnormalities including junctional rhythm and altered P-wave morphologies (Fig. 6C) were recorded with significantly greater frequency in Tg26-hDMPK compared with the electrically more stable WT (Fig. 6D). Thus, overexpression of *hDMPK* produces features of hypertrophic maladaptive cardiomyopathy with dysrhythmia, recapitulating typical cardiac features in myotonic dystrophy (2,38).

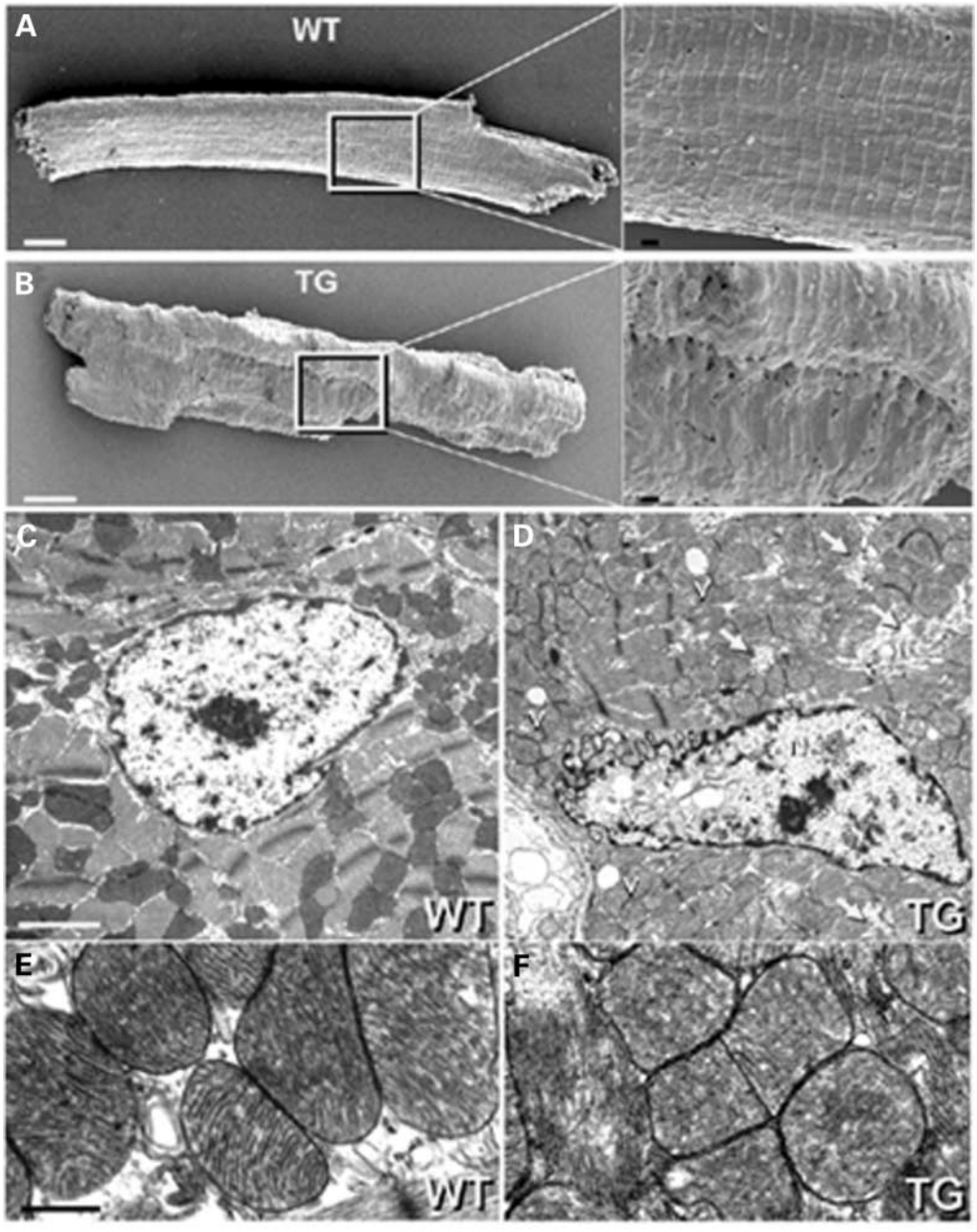

Figure 5. Degenerated Tg26-hDMPK (TG) cardiomyocytes. (**A** and **B**) Left, Distorted cytoarchitecture of TG (B) versus regular rod-shaped WT (A) ventricular cardiomyocytes on field emission scanning electron microscopy; bars: 10 μm. Right, Higher resolution of individual cell surface displaying abnormal sarcomeric organization in TG (lower) versus WT (upper); bars: 1 μm. (**C** and **D**) Transmitted electron microscopy of the perinuclear area of a normal WT cardiomyocyte demonstrates compact sarcomeric organization surrounding a well-defined nucleus (C) versus a TG cardiomyocyte with myofibrillar degeneration (arrow), blebbed nucleus (N) and nuclear/cytosolic vacuoles (v) (D). Bar in C: 2 μm, also for D. (**E** and **F**) Numerous and well-defined cristae in mitochondria from WT (E) versus abnormal mitochondrial matrix with poorly delineated cristae in TG (F). Bar in E: 500 nm, also for F.

Myotonic myopathy in the *hDMPK* overexpressor

Myotonia, another key feature of myotonic dystrophy, is characterized by hyperexcitability of skeletal muscle following voluntary contractions, percussion or mechanical stimulation with needle insertion, and has been associated with a deficit in sarcolemmal chloride channels (39–41). Disruption of normal skeletal muscle function was here indicated *in vivo* by sporadic yet dramatic transient episodes of walking difficulties observed in the ambulatory Tg26-hDMPK mouse (Fig. 7A). On needle electromyography, under light anesthesia, needle insertion triggered prolonged myotonic discharges characterized by high frequency repetitive potentials, regularly recorded from distal limb muscles in Tg26-hDMPK mice with a prevalence of 83% ($n = 6$), but seldom seen in WT (27%, $n = 11$; Fig. 7B). Compared with positive immunofluorescent staining of the sarcolemma from WT tibialis cranialis and gastrocnemius soleus, the Tg26-hDMPK

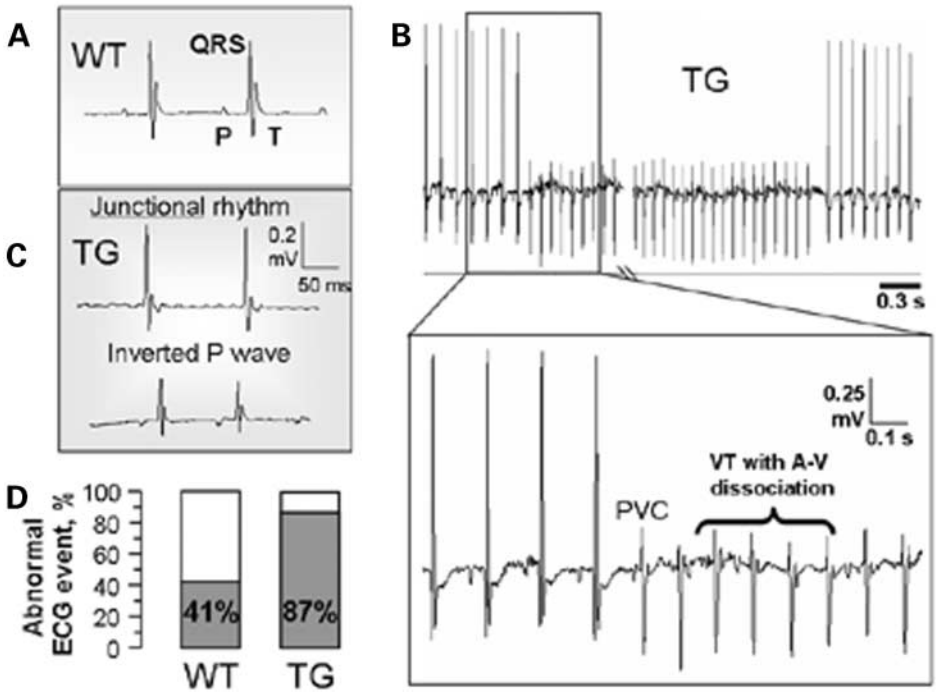

Figure 6. Abnormal ECG and dysrhythmia in Tg26-hDMPK (TG). In contrast to normal sinus rhythm recorded from awake ambulatory WT (**A**), episodes of tachyarrhythmia were commonly seen in TG (**B**), characterized by premature ventricular beats (PVC) with the development of ventricular tachyarrhythmia (VT) and atrio-ventricular (AV) dissociation (inset). (**C** and **D**) A spectrum of ECG abnormalities, including junctional rhythm and inverted P waves (C), frequent in TG compared with WT (D).

showed a pronounced deficit in the sarcolemmal chloride ClC-1 channel (Fig. 7C and D), a voltage-dependent channel population responsible for the electrical stability of skeletal muscle (39). Moreover, light microscopy of Gomori's trichrome-stained skeletal muscle sections revealed the presence of ragged fibers in Tg26-hDMPK, not observed in WT specimens (Fig. 8A). Such torn fibers in the Tg26-hDMPK displayed abundant red staining that accounts for accumulation of mitochondria in the subsarcolemmal space and between myofibrils, a further marker of myopathy (39). Compared with WT ($n = 3$), the Tg26-hDMPK ($n = 4$) demonstrated a >2-fold increase in the number of skeletal muscle fibers with central nuclei, i.e. 6.3 ± 1.6 versus 2.6 ± 0.4 ($P = 0.007$; Fig. 8B and C), indicative of cytoskeleton malfunction and/or degeneration in dystrophic muscle. In addition, a broad spectrum of fiber sizes was detected in Tg26-hDMPK compared with a more uniform normal distribution in the WT. The observed fiber heterogeneity in the Tg26-hDMPK ($n = 4$) translated into a 4-fold greater ratio of largest over smallest fiber size compared with WT ($n = 4$), i.e. 14 ± 4 versus 3 ± 1 respectively ($P = 0.03$; Fig. 8B and D), indicating atrophy of type I with moderate hypertrophy of type II fibers (2). This was further apparent on ultrastructural analysis of the Tg26-hDMPK skeletal muscle which prominently demonstrated central nuclei, ringed fibers, hypotrophy with sarcomeric disorganization and sarcoplasmic masses, all distinctive signs of the myopathic state (2,42), in contrast to the regular sarcomeric structure of the WT with peripheral nuclei (Fig. 8E). The ringed fibers of the Tg26-hDMPK, with the outer ring of myofibrils running perpendicularly to the rest of myofibrils in the same muscle fiber, regularly demonstrated abnormal nuclei with irregular nuclear membranes, as well as sarcoplasmic areas where normal myofibrillar organization was replaced by aggregation of tubules with numerous free ribosomes and scattered bundles of myofilaments, not observed in the WT (Fig. 8E and insets). Thus, *hDMPK* overexpression alters the normal skeletal muscle phenotype.

Arterial tone deficit in the *hDMPK* overexpressor

Proper arterial smooth muscle tone is a principal determinant of systemic blood pressure. Here, automated blood pressure monitoring in awake mice revealed depressed systemic systolic and diastolic arterial pressure in the Tg26-hDMPK compared with WT (Fig. 9A and B), a vascular sign of myotonic dystrophy (2). On average, mean arterial pressure was 126 ± 5 mmHg versus 109 ± 5 mmHg in WT ($n = 10$) and Tg26-hDMPK ($n = 10$), respectively ($P < 0.02$; Fig. 9C). This deficit in systemic pressure in the Tg26-hDMPK was confirmed by direct intra-arterial measurement under anesthesia (Fig. 9C inset), and was recorded at similar heart rates with WT (Fig. 9D). Thus, overexpression of *hDMPK* gene products disrupts not only cardiac and skeletal muscle homeostasis, but also smooth muscle function translating into compromised regulation of the systemic cardiovascular state.

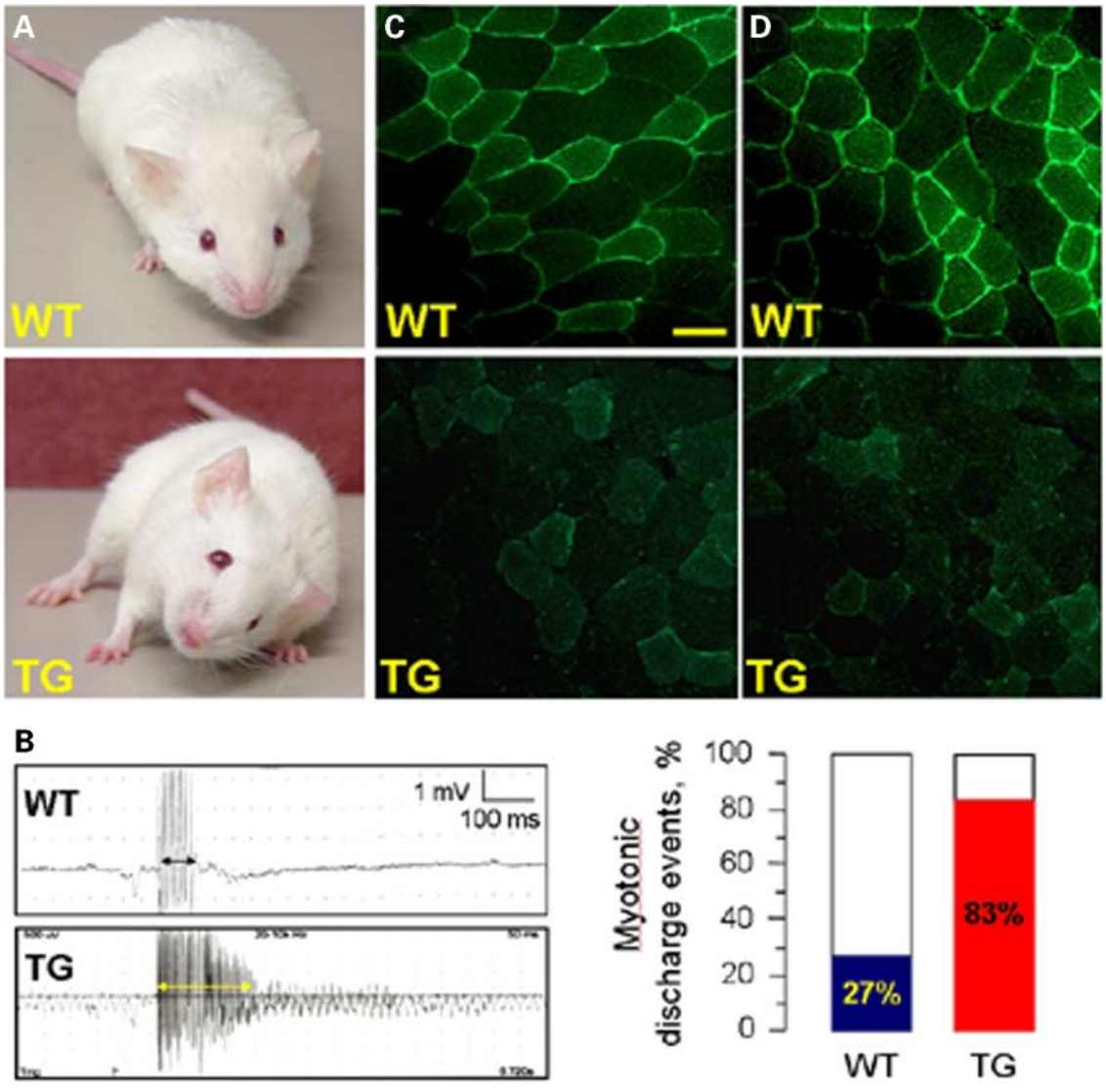

Figure 7. Myotonic myopathy with reduced ClC-1 chloride channel expression in Tg26-hDMPK (TG) skeletal muscle. (**A**) Episode of walking impairment in TG compared with normal gait of the WT. (**B**) On electromyography (EMG) of distal limb muscles where normal EMG electrode insertional activity is observed in WT, electrode insertion triggers myotonic discharges in TG myofibers. These high frequency repetitive potentials triggered by motor unit stimulation (yellow versus black arrow; left) translated into an overall higher incidence of myotonic discharges in TG compared with WT (right). (**C** and **D**) Anti-ClC-1 antibody-based immunofluorescence of transverse cryosections of tibialis cranialis (C) and gastrocnemius soleus (D) reveals a reduction in sarcolemmal chloride channel protein in TG (bottom) compared with prominent sarcolemmal chloride channel in the WT (top). Bar in C: 50 μm, also for D.

DISCUSSION

This first phenotypic characterization of an older murine model engineered to overexpress the human *DMPK* gene demonstrates that persistent output of *DMPK* gene products, resulting in a continuous surplus of hDMPK transcripts with a $(CUG)_{11}$ repeat and hDMPK protein isoforms above the endogenous levels of DMPK mRNA and protein, causes severe cellular distress. Cumulated through development, growth and aging, the *hDMPK* overexpression-triggered distress produced an integral pathophysiological phenotype that recapitulated key systemic muscle features of myotonic dystrophy seen in DM1 patients. The age-related impact of stress accumulation, determined here in the 11–15 months old animal, revealed reduced workload tolerance associated with overt cardiomyopathic remodeling, myotonic myopathy and arterial tone deficit as most prominent features in this Tg26-hDMPK transgenic overexpressor line. As transgene-copy-number dependent and transgene-integration-site independent milder features of this phenotype develop earlier in the lifespan of related transgenic lineages (9), the present findings strongly suggest that the uncompensated compromise in the structure and function of muscle systems in the Tg26-hDMPK is elicited by excessive expression level, albeit typical distribution, of gene products from the hDMPK transgene. Taken together, these data underscore a vital role for proper DMPK expression in securing adequate muscle operation.

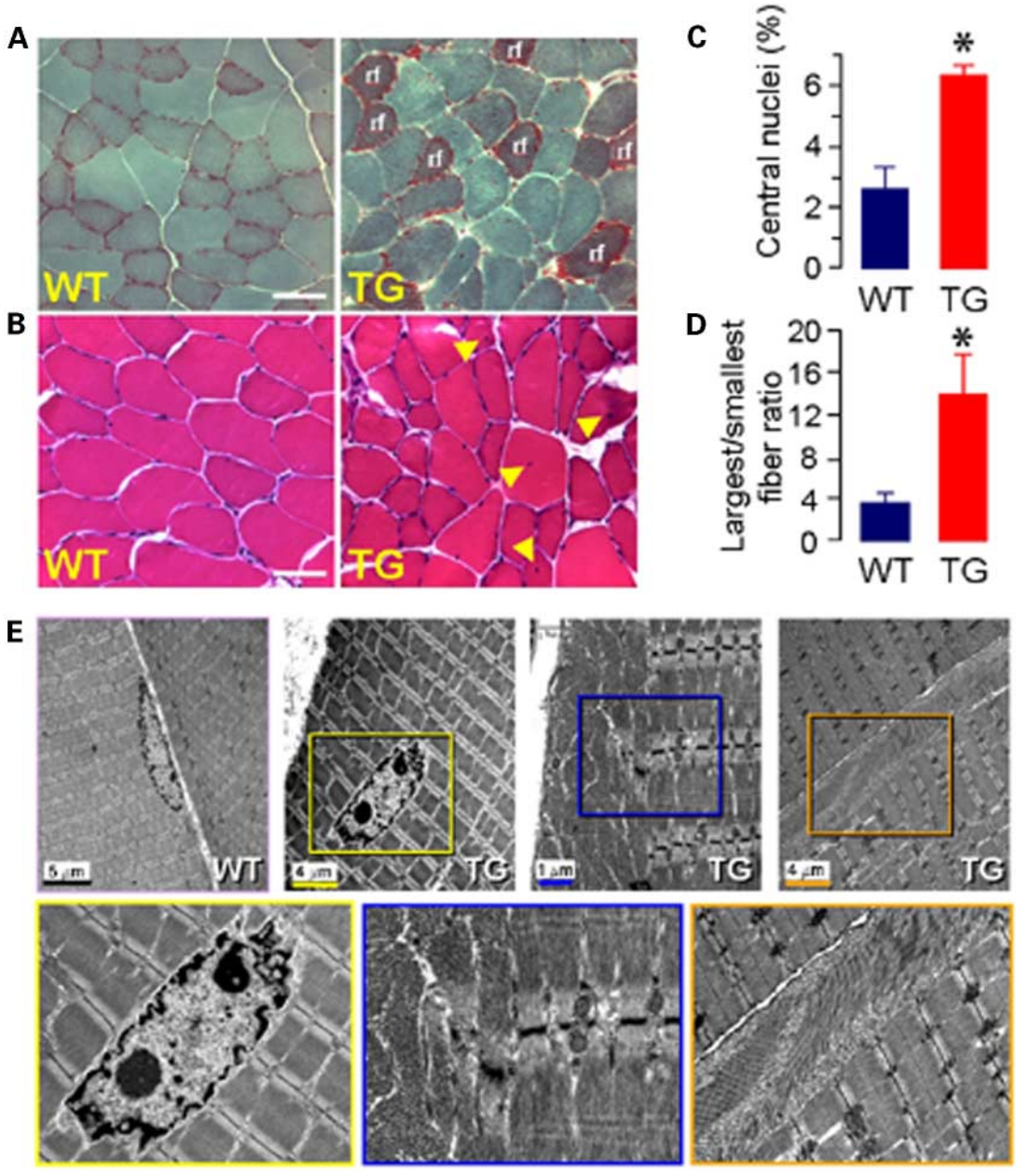

Figure 8. Abnormal structure of Tg26-hDMPK (TG) skeletal muscle. (**A**) Under light microscopy, prominent staining with Gomori's trichrome of mitochondria in skeletal muscle sections is evident in TG, characteristic of ragged fibers (rf), and not observed in WT; bar: 50 μm. (**B**–**D**) Compared with WT, TG shows a >2-fold increase in the number of central skeletal muscle nuclei (arrows heads in B and average values in C), in addition to a 4-fold variation in fiber size ratio (D); bar: 50 μm. (**E**) In TG, electron microscopy further shows central nuclei (TG left), ringed fiber appearance (TG middle) and sarcoplasmic aggregates (TG right), all typical for a myopathic state, compared with normal WT. Insets: Magnified selected areas from paired-colored TG specimens highlighting the centralized nucleus with irregular membranes (left), ringed fibers with perpendicular myofibrils (middle) and tubular aggregates with free ribosomes and scattered myofilaments (right).

Important in the interpretation of present findings is the notion that *hDMPK* gene products are generated in substantial amounts only in muscle tissues (33). In line with the tissue-specific prevalence, Tg26-hDMPK demonstrated particular overexpression in all muscle types. Subcellularly, DMPK protein partitions in an isoform-dependent manner within the mitochondria and cytosol, as well as the endoplasmic reticulum, at least in some species (5,33). Localizations to gap junctions and intercalated disks in (heart) muscle tissue have also been reported (43). Although the actual targets of DMPK-dependent phosphorylation remain largely unknown, DMPK has been implicated, on the basis of the identification of the myosin phosphatase regulatory subunit as its binding partner, in the modulation of the contraction–relaxation cycle and organelle motility by setting cytoskeletal dynamics (5,20,33,44). Moreover, DMPK has been involved in

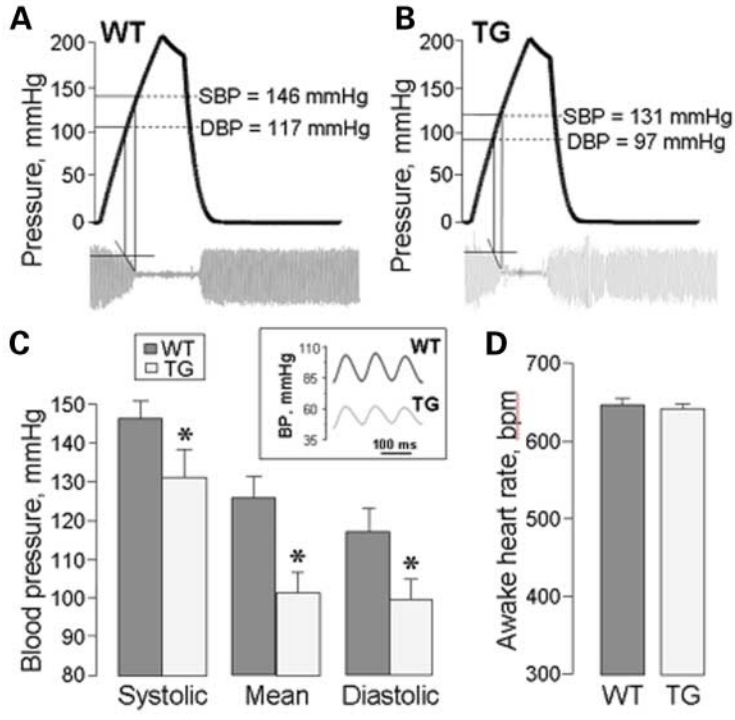

Figure 9. Deficit in arterial smooth muscle tone leads to lower blood pressure in Tg26-hDMPK (TG). (**A**–**C**) Tail-cuff monitoring of systemic blood pressure in WT (A) and TG (B) mice reveals lower systolic, diastolic and mean blood pressures in awake TG compared with WT and confirmed under anesthesia (C inset), without significant difference in heart rate (**D**).

intracellular calcium and chloride handling (16). Thus, the present demonstration of multisystemic and severe alterations in the aged Tg26-hDMPK underscores, at the whole organism level, the broad involvement of DMPK-mediated signaling in orchestrating muscle homeostasis.

Senescence predisposes to progressive reduction in the adaptive capacity of the body, in particular of muscle systems, to diverse and metabolically demanding stress loads (45,46). In contrast to the young animal that displays a mild phenotype in response to abnormal expression of *hDMPK* gene products corresponding to an initial phase of disease (9), the poor physical tolerance to imposed workload in the aged hDMPK overexpressor recapitulates the stress-intolerant behavior of established transgenic models of metabolic sensor deficiency (47,48), and implicates normal DMPK expression in optimal body performance.

In the heart, gross changes in the size of the myocardium with derangements in the architecture of cardiomyocytes are highly indicative of cardiac maladaptation with the magnitude of LV mass denoting the severity of structural alterations (35–37). Here, hypertrophic cardiomyopathy affecting the left ventricle in Tg26-hDMPK was further associated with prominent interstitial fibrosis that correlated with structural remodeling. With overexpression of DMPK, the highly organized sarcomeric ultrastructure of the cardiomyocyte was lost, and replaced by myofibrillar degeneration, distorted nuclei and disrupted mitochondrial cristae, all histopathological features typical of patients with DM1 (49). As aberrant myocardial calcium handling is a principle modulator of intracellular hypertrophic signaling with intracellular calcium overload associated with poor outcome (50), excessive accumulation of calcium in Tg26-hDMPK cardiomyocytes may provide a molecular basis underlying cardiac disturbances. NFAT, the calcium-activated master cardiac transcription factor implicated in pro-hypertrophic genetic cardiac reprograming (36), was found here translocated into the nucleus of Tg26-hDMPK cardiomyocytes. Such cytosolic/nuclear shuttling is a prerequisite for NFAT activity and the resulting hypertrophic phenotype (35–37). Furthermore, as in patients with DM1 (49) and in line with the reported role of DMPK in regulating cardiac electrical conduction (10), an increased incidence of abnormal electrophysiological activity was captured in Tg26-hDMPK. Thus, hearts overexpressing *hDMPK* display features of hypertrophic cardiomyopathy with predisposition for dysrhythmia seen regularly in patients with clinically confirmed DM1 (2), implicating thereby that proper regulation of DMPK expression is essential for the maintenance of cardiac structure and function.

A further sign of DM1 is the delayed relaxation of skeletal muscle following contraction or stiffness, known as myotonia, which is due to hyperexcitability of fibers leading to repetitive action potentials and involuntary after-contractions (51). Tg26-hDMPK episodically showed transient 'stiffness' with gait disturbance and frequent myotonic discharges. Though myotonia was prominent and present in almost all of the Tg26-hDMPK, a few WT also displayed discharges, in line with reports of false positive electromyographic findings in certain normal subjects (52). Myotonic discharges in DM1 have been linked to loss of the muscle-specific chloride channel ClC-1 (18), and accordingly a major depletion of

ClC-1 protein in the sarcolemma of Tg26-hDMPK was observed. On differential diagnosis by histology, active degeneration or necrosis was ruled out in Tg26-hDMPK skeletal muscle. Rather, the intracellullar changes observed, including an increased number of centrally placed nuclei, are amongst the most common and typical findings in DM1 that often occur before other significant muscle signs can be recognized in the clinical setting (2). In addition, variation in fiber size, evident sarcoplasm masses and the presence of ringed fibers in Tg26-hDMPK are all considered highly specific markers of myotonic dystrophy, and are rarely seen in other muscle disorders (42). Although not individually pathognomonic for myotonic dystrophy, the combined presentation of such multiple histological and ultrastructural changes in the present model of *hDMPK* overexpression fulfills all the established criteria for the skeletal muscle phenotype of myotonic dystrophy (2).

In line with the DMPK predilection for all muscle types (33), *hDMPK* overexpression in the smooth muscle translated into a compromised systemic arterial tone. Such deficit in smooth muscle function and the associated lowering of blood pressure recorded in Tg26-hDMPK is in accord with systemic hypotension recognized in patients with DM1 as a most typical and frequent cardiovascular manifestation of the disease state (53,54).

Despite similarities with the Tg26-hDMPK phenotype, in patients with DM1 it is expression of the only known natural-mutant form of the *hDMPK* gene, i.e. a gene with an expanded $(CTG)_n$ repeat insert in the last non-coding 15th exon, that causes the complex multisystemic and progressive pathology of the disease state (21–24). This is somewhat distinct from the Tg26-hDMPK mouse model presented here as the transgene used produces a normal hDMPK mRNA with a normal-sized $(CUG)_{11}$ repeat tract, encoding the full complement of alternatively spliced DMPK isoforms. Moreover, in patients with classical DM1 there is no evidence in support of overexpression of hDMPK at the protein level (6). Instead, accumulating evidence supports a determining role for nuclear build-up of abnormal levels of expanded $(CUG)_n$ repeat containing RNA, with mechanistic features shared between various expansion disorders (30,31). Thus, at least in principle, the continuous presence of a too high copy number of hDMPK mRNA with a $(CUG)_{11}$ repeat in the Tg26-hDMPK could mimic the condition of DM1 patients with (sub)normal dose of hDMPK mRNAs with an expanded $(CUG)_n$ repeat, suggesting that the overall dose of the CUG-triplets present in repeats and not the number or length of individual repeat tracts precipitates the phenotype. In this regard, it has been shown that stress modulates the stability of CNG repeats (55). In fact, transgenic overexpression of the hDMPK 3′-UTR with $(CUG)_{11}$ repeats interferes with normal myogenesis, indicating that overexpression of normal hDMPK mRNA (or parts thereof) *per se* is not neutral (27). Alternatively, continuous overexpression of the hDMPK protein in Tg26-hDMPK may elicit an ensemble of cellular challenges equivalent to those occurring with abnormal RNA. Though the present study does not discriminate between these two possibilities, the normal $(CUG)_{11}$ length present in the Tg26-hDMPK is considered not to be amenable in readily forming base-paired hairpins or in driving excessive binding of RNA to proteins, in clear contrast to RNAs with extended repeat lengths of (CUG) which are prone to pathologic RNA folding as proposed for DM1 (29,56,57). In fact, longer CNG hairpins form quickly and dissociate slowly compared with short repeats (58). Conversely, overexpression of hDMPK *per se* has been shown to trigger pathogenic effects (59), suggestive of a direct role for hDMPK protein-based stress in the pathobiology of Tg26-hDMPK.

In conclusion, accumulated distress derived with age from continuous overexpression of *hDMPK* precipitates maladaptation in muscle systems, generating pathologic hypertrophic cardiomyopathy with dysrhythmia, myotonic skeletal muscle myopathy and smooth muscle tone deficit with systemic hypotension. In this way, the exercise-intolerant Tg26-hDMPK model with approximately 25 copies of otherwise normal *hDMPK* recapitulates key traits of DM1 tested in muscle systems. Thus, the Tg26-hDMPK line is here established as a useful tool in evaluating the effects of cumulative molecular stress related to the overactivity of hDMPK protein isoforms in cells of all muscle types in the context of augmented doses of (CUG)-triplets in normal-sized repeats in *hDMPK* mRNAs. *DMPK*, thereby, plays a vital homeostatic role in support of the muscular wellbeing maintaining coordinated structure and function.

MATERIALS AND METHODS

Transgenic *hDMPK* overexpressor mouse line

A ~14 kb *Nhe*I genomic fragment containing all human *DMPK* (*hDMPK*) exons, along with the last exon of the upstream *DMWD* gene, was incorporated into the mice germline by conventional transgenesis (9). WT females were bred with transgenic males over more than 20 generations. Resultant heterozygous transgenic offsprings, named Tg26-hDMPK, were identified by tail-cut PCR and compared with age-matched 11 to 15-month-old WT littermates. Protocols were approved by the Mayo Foundation and Nijmegen Center for Molecular Life Sciences Institutional Animal Care and Use Committees.

Northern and western blot analysis

Northern blot analysis of RNA isolated from heart, skeletal and smooth muscles, as well as brain and liver, was performed in parallel from WT and Tg26-hDMPK specimens. Blots were hybridized with a DMPK probe, a mixture of mouse and human full length *DMPK* cDNAs. RNA loading was verified by ethidium bromide staining of 28S rRNA and hybridization with a GAPDH probe. For western blot analysis, whole tissue lysates were incubated with the B79 polyclonal anti-DMPK antibody (7). As a control, specimens from a DMPK-null ($DMPK^{-/-}$) mouse (9) were compared.

Treadmill stress test

WT and Tg26-hDMPK mice were simultaneously exercised on a two-track treadmill (Columbus Instruments, Columbus,

OH) with a graded protocol of increasing incline or velocity at 3 min intervals (34,48). Tolerated workload (J) was used as a parameter of performance, and defined by the sum of kinetic ($E_k = mv^2/2$) andpotential ($E_p = mgvt \sin\theta$) energy, where m represents animal mass, v running velocity, g acceleration due to gravity, t elapsed time at a protocol level and θ angle of incline.

Echocardiography

Cardiac ultrasound was performed in lightly sedated (1% isoflurane) WT and Tg26-hDMPK mice, with a 15L8 transducer interfaced with a Sequoia 512 echocardiography platform (Siemens, Malvern, PA). M-mode images were digitally acquired and stored for off-line blinded analysis. Echocardiographic measurements of LV dimensions were recorded at end-diastole and end-systole from three consecutive cardiac cycles using the leading edge method (34).

Histochemistry and laser confocal microscopy

WT and Tg26-hDMPK myocardium were fixed in 10% buffered formalin, and 0.5 μm-thick sections of paraffin-embedded cardiac muscle samples were stained with Masson's trichrome for microscopic evaluation of interstitial fibrosis. Alternatively, isolated cardiac cells (47) were either loaded with the calcium-fluorescent probe Fluo-3 for imaging of cytosolic calcium (48) or fixed (with 3% paraformaldehyde) for immunofluorescence of the cardiac transcription factor NFAT3 (Santa Cruz Biotechnology; 34). Concomitantly, 5 μm thick sections of flash-frozen skeletal muscle specimens were processed for histochemistry using hematoxylin/eosin or Gomori's trichrome (60) or 6 μm thick cryosections of tibialis cranialis and gastrocnemius soleus were immunoprobed with a polyclonal anti-ClC1 chloride channel antibody (Alomone Labs, Jerusalem, Israel). Histology was performed on an Axioplan 2 light microscope fitted with an Axiocam digital camera (Carl Zeiss MicroImaging, Thornwood, NY). Calcium imaging and immunofluorescence were acquired with a Zeiss LSM 510 confocal microscope. Digital images were analyzed with the Metamorph software (Visitron Universal Imaging, Downingtown, PA).

Transmitted and field-emission scanning electron microscopy

WT and Tg26-hDMPK cardiac and skeletal muscle tissue or isolated cardiomyocytes were fixed in phosphate buffered saline (PBS) with 1% glutaraldehyde and 4% formaldehyde (pH 7.2). For transmitted electron microscopy, samples were processed in phosphate-buffered 1% OsO_4, stained with 2% uranyl acetate, dehydrated in ethanol and propylene oxide and embedded in epoxy resin. Thin (90 nm) sections were placed on copper grids, stained with lead citrate and micrographs were taken with a JEOL 1200 electron microscope (JEOL Ltd, Tokyo, Japan). For field-emission scanning electron microscopy, fixed cardiomyocytes were rinsed in PBS with 1% osmium, dehydrated with ethanol and dried in a critical Ted Pella point dryer (61). On coating with platinum using an Ion Tech indirect argon ion voltage of 9.5 kV and 4.2 mA, samples were examined at accelerating voltage (1.0, 2.4, 3.5 and 5.0 kV) on a Hitachi 4700 scanning microscope (62).

ECG and telemetry

Twelve-lead ECG recordings were obtained in 1% isoflurane-anesthetized WT and Tg26-hDMPK mice. Electrodes were placed subcutaneously in all four distal limbs and in the precordial region in an Einthoven configuration (63,64). Signals from all configurations were acquired at 11.8 kHz (Instrutech, Long Island NY) and amplified by an ECG amplifier (Gould Electronics, Eastlake, OH). In ambulatory mice, continuous electrographic recordings were obtained from implanted telemetry devices (Data Sciences International, St. Paul, MN; 48). Transmitters were placed in the peritoneal cavity and leads were tunneled subcutaneously in a lead II configuration under isoflurane anesthesia. Electrocardiogram signals were acquired at 2 kHz, 2 weeks post-surgery.

Electromyography

Needle electromyography (Viking IV, Nicolet Biomedical, Madison, WI) was carried out on WT and Tg26-hDMPK mice, by the investigator blinded to mouse type, in order to assess the electrical activity of gastrocnemius, tibialis cranialis and wrist extensor muscles. All skeletal muscle were explored at rest under light sedation (isoflurane 1%) using a 30-gauge concentric needle electrode (Medtronic Functional Diagnostics A/S, Denmark). Potentials were digitally recorded and stored for off-line retrieval of waveforms.

Blood pressure recording

Following 1-week of acclimatization, blood pressure was measured by automated tail-cuff recording (Columbus Instruments) in awake restrained WT and Tg26-hDMPK mice. Systolic and diastolic values were derived from 10 sequential recordings. In addition, intra-arterial blood pressure measurements were obtained directly by a 1.4-Fr micro-pressure catheter (SPR-671, Millar Instruments) following carotid arterial cannulation under 1.5% isoflurane (1 l/min air) anesthesia.

Statistical analysis

Data are expressed as mean ± SEM. Comparisons are by paired Student's t-test or analysis of variance. $P < 0.05$ was pre-determined. Analysis was performed using the JMP software (SAS Institute Inc., Cary, NC).

ACKNOWLEDGEMENTS

We thank, at the Mayo Clinic, Dr A.G. Engel for expert discussion and review of pathologic muscle specimens, and the Translational Ultrasound Research Core for use of the echocardiographic machine. This work was supported by the National Institutes of Health (HL64822, GM08685,

GM65841, HL07111), Mayo Foundation Clinician–Investigator Program, MayoCR20 Research Program, American Heart Association, Miami Heart Research Institute, Mayo Clinic Marriott Heart Disease Research Program, Marriott Foundation, Mayo–Dubai Healthcare City Research Project, Muscular Dystrophy Association, Association Contre les Myopathies and the Prinses Beatrix Fonds. A.T. is an Established Investigator of the American Heart Association.

REFERENCES

1. Manning, G., Whyte, D.B., Martinez, R., Hunter, T. and Sudarsanam, S. (2002) The protein kinase complement of the human genome. *Science*, **298**, 1912–1934.
2. Harper, P.S. (2001) *Myotonic Dystrophy*. WB Saunders Co Ltd, London, UK.
3. Riento, K. and Ridley, A.J. (2003) Rocks: multifunctional kinases in cell behaviour. *Nat. Rev. Mol. Cell. Biol.*, **4**, 446–456.
4. Ueda, H., Ohno, S. and Kobayashi T. (2000) Myotonic dystrophy and myotonic dystrophy protein kinase. *Prog. Histochem. Cytochem.*, **35**, 187–251.
5. Wansink, D.G., van Herpen, R.E.M.A., Coerwinkel-Driessen, M.M., Groenen, P.J.T.A., Hemmings, B.A. and Wieringa, B. (2003) Alternative splicing controls myotonic dystrophy protein kinase structure, enzymatic activity and subcellular localization. *Mol. Cell. Biol.*, **23**, 5489–5501.
6. Wansink, D.G. and Wieringa, B. (2003) Transgenic mouse models for myotonic dystrophy type 1 (DM1). *Cytogenet. Genome Res.*, **100**, 230–242.
7. Groenen, P.J.T.A., Wansink, D.G., Coerwinkel, M., van den Broek, W., Jansen, G. and Wieringa, B. (2000) Constitutive and regulated modes of splicing produce six major myotonic dystrophy protein kinase (DMPK) isoforms with distinct properties. *Hum. Mol. Genet.*, **9**, 605–616.
8. Jansen, G., Mahadevan, M., Amemiya, C., Wormskamp, N.G., Segers, B., Hendriks, W., O'Hoy, K., Baird, S., Sabourin, L., Lennon, G. *et al.* (1992) Characterization of the myotonic dystrophy region predicts multiple protein isoforms-encoding mRNAs. *Nat. Genet.*, **1**, 261–266.
9. Jansen, G., Groenen, P.J.T.A., Bachner, D., Jap, P.H., Coerwinkel, M., Oerlemans, F., van den Broek, W., Gohlsch, B., Pette, D., Plomp, J.J. *et al.* (1996) Abnormal myotonic dystrophy protein kinase levels produce only mild myopathy in mice. *Nat. Genet.*, **13**, 316–324.
10. Berul, C.I., Maguire, C.T., Aronovitz, M.J., Greenwood, J., Miller, C., Gehrmann, J., Housman, D., Mendelsohn, M.E. and Reddy, S. (1999) DMPK dosage alterations result in atrioventricular conduction abnormalities in a mouse myotonic dystrophy model. *J. Clin. Invest.*, **103**, R1–R7.
11. Mounsey, J.P., Mistry, D.J., Ai, C.W., Reddy, S. and Moorman, J.R. (2000) Skeletal muscle sodium channel gating in mice deficient in myotonic dystrophy protein kinase. *Hum. Mol. Genet.*, **9**, 2313–2320.
12. Pall, G.S., Johnson, K.J. and Smith, G.L. (2003) Abnormal contractile activity and calcium cycling in cardiac myocytes from DMPK-KO mice. *Physiol. Genomics*, **13**, 139–146.
13. Lee, H.C., Patel, M.K., Mistry, D.J., Wang, Q., Reddy, S., Moorman, J.R. and Mounsey, J.P. (2003) Abnormal Na channel gating in murine cardiac myocytes deficient in myotonic dystrophy protein kinase. *Physiol. Genomics*, **12**, 1471–1475.
14. Steinmeyer, K., Klocke, R., Ortland, C., Gronemeier, M., Jockusch, H., Grunder, S. and Jentsch, T.J. (1991) Inactivation of muscle chloride channel by transposon insertion in myotonic mice. *Nature*, **354**, 304–308.
15. Mounsey, J.P., Xu, P., John, J.E., III, Horne, L.T., Gilbert, J., Roses, A.D. and Moorman, J.R. (1995) Modulation of skeletal muscle sodium channels by human myotonin protein kinase. *J. Clin. Invest.*, **95**, 2379–2384.
16. Benders, A.G.M., Groenen, P.J.T.A., Oerlemans, F.T.J.J., Veerkamp, J.H. and Wieringa, B. (1997) Myotonic dystrophy protein kinase is involved in the modulation of the Ca^{2+} homeostasis in skeletal muscle cells. *J. Clin. Invest.*, **100**, 1440–1447.
17. Kimura, T., Takahashi, M.P., Okuda, Y., Kaido, M., Fujimura, H., Yanagihara, T. and Sakoda, S. (2000) The expression of ion channel mRNAs in skeletal muscles from patients with myotonic muscular dystrophy. *Neurosci. Lett.*, **295**, 93–96.
18. Mankodi, A., Takahashi, M.P., Jiang, H., Beck, C.L., Bowers, W.J., Moxley, R.T., Cannon, S.C. and Thornton C.A. (2002) Expanded CUG repeats trigger aberrant splicing of ClC-1 chloride channel pre-mRNA and hyperexcitability of skeletal muscle in myotonic dystrophy. *Mol. Cell.*, **10**, 35–44.
19. Jin, S., Shimizu, M., Balasubramanyam, A. and Epstein, H.F. (2000) Myotonic dystrophy protein kinase (DMPK) induces actin cytoskeletal reorganization and apoptotic-like blebbing in lens cells. *Cell Motil. Cytoskeleton*, **45**, 133–148.
20. Muranyi, A., Zhang, R., Liu, F., Hirano, K., Ito, M., Epstein, H.F. and Hartshorne, D.J. (2001) Myotonic dystrophy protein kinase phosphorylates the myosin phosphatase targeting subunit and inhibits myosin phosphatase activity. *FEBS Lett.*, **493**, 80–84.
21. Fu, Y.H., Pizzuti, A., Fenwick, Jr, R.G., King, J., Rajnarayan, S., Dunne, P.W., Dubel, J., Nasser, G.A., Ashizawa, T., de Jong, P. *et al.* (1992) An unstable triplet repeat in a gene related to myotonic muscular dystrophy. *Science*, **255**, 1256–1258.
22. Brook, J.D., McCurrach, M.E., Harley, H.G., Buckler, A.J, Church, D., Aburatani, H., Hunter, K., Stanton, V.P., Thirion, J.P., Hudson, T. *et al.* (1992) Molecular basis of myotonic dystrophy: expansion of a trinucleotide (CTG) repeat at the 3′ end of a transcript encoding a protein kinase family member. *Cell*, **68**, 799–808.
23. Mahadevan, M., Tsilfidis, C., Sabourin, L., Shutler, G., Amemiya, C., Jansen, G., Neville, C., Narang, M., Barcelo, J., O'Hoy, K. *et al.* (1992) Myotonic dystrophy mutation: an unstable CTG repeat in the 3′ untranslated region of the gene. *Science*, **255**, 1253–1255.
24. Aslanidis, C., Jansen, G., Amemiya, C., Shutler, G., Mahadevan, M., Tsilfidis, C., Chen, C., Alleman, J., Wormskamp, N.G., Vooijs, M. *et al.* (1992) Cloning of the essential myotonic dystrophy region and mapping of the putative defect. *Nature*, **355**, 548–551.
25. Sabourin, L.A., Tamai, K., Narang, M.A. and Korneluk, R.G. (1997) Overexpression of 3′-untranslated region of the myotonic dystrophy protein kinase cDNA inhibits myoblast differentiation *in vitro*. *J. Biol. Chem.*, **272**, 29626–29635.
26. Furling, D., Lam le, T., Agbulut, O., Butler-Browne, G.S. and Morris, G.E. (2003) Changes in myotonic dystrophy protein kinase levels and muscle development in congenital myotonic dystrophy. *Am. J. Pathol.*, **162**, 1001–1009.
27. Storbeck, C.J., Drmanic, S., Daniel, K., Waring, J.D., Jirik, F.R., Parry, D.J., Ahmed, N., Sabourin, L.A., Ikeda, J. and Korneluk, R.G. (2004) Inhibition of myogenesis in transgenic mice expressing the human DMPK 3′-UTR. *Hum. Mol. Genet.*, **13**, 589–600.
28. Amack, J.D. and Mahadevan, M.S. (2004) Myogenic defects in myotonic dystrophy. *Dev. Biol.*, **265**, 294–301.
29. Ebralidze, A., Wang, Y., Petkova, V., Ebralidse, K. and Junghans, R.P. (2004) RNA leaching of transcription factors disrupts transcription in myotonic dystrophy. *Science*, **303**, 383–387.
30. Ranum, L.P. and Day, J.W. (2004) Myotonic dystrophy: RNA pathogenesis comes into focus. *Am. J. Hum. Genet.*, **74**, 793–804.
31. La Spada, A.R., Richards, R.I. and Wieringa, B. (2004) Dynamic mutations on the move in Banff. *Nat. Genet.*, **36**, 667–670.
32. Storbeck, C.J., Sabourin, L.A., Waring, J.D. and Korneluk, R.G. (1998) Definition of regulatory sequence elements in the promoter region and the first intron of the myotonic dystrophy protein kinase gene. *J. Biol. Chem.*, **273**, 9139–9147.
33. Lam, L.T., Pham, Y.C., Nguyen, T.M. and Morris, G.E. (2000) Characterization of a monoclonal antibody panel shows that the myotonic dystrophy protein kinase, DMPK, is expressed almost exclusively in muscle and heart. *Hum. Mol. Genet.*, **9**, 2167–2173.
34. Kane, G.C., Behfar, A., Yamada, S., Perez-Terzic, C., O'Cochlain, F., Reyes, S., Dzeja, P.P., Miki, T., Seino, S. and Terzic, A. (2004). K_{ATP} channel knockout compromises the metabolic benefit of exercise training resulting in cardiac deficits. *Diabetes*, in press.
35. Chien, K.R. (1999) Stress pathways and heart failure. *Cell*, **98**, 555–558.
36. Frey, N. and Olson, E.N. (2003) Cardiac hypertrophy: the good, the bad, and the ugly. *Annu. Rev. Physiol.*, **65**, 45–79.
37. Chien, K.R. and Olson, E.N. (2002) Converging pathways and principles in heart development and disease. *Cell*, **110**, 153–162.
38. Wieringa, B. (1994) Myotonic dystrophy reviewed: back to the future? *Hum. Mol. Genet.*, **3**, 1–7.
39. Gurnett, C.A., Kahl, S.D., Anderson, R.D. and Campbell, K.P. (1995) Absence of the skeletal muscle sarcolemma chloride channel ClC-1 in myotonic mice. *J. Biol. Chem.*, **270**, 9035–9038.

40. Charlet-B., N., Savkur, R.S., Singh, G., Philips, A.V., Grice, E.A. and Cooper, T.A. (2002) Loss of the muscle-specific chloride channel in type 1 myotonic dystrophy due to misregulated alternative splicing. *Mol. Cell.*, **1**, 45–53.
41. Kanadia, R.N., Johnstone, K.A., Mankodi, A., Lungu, C., Thornton, C.A., Esson, D., Timmers, A.M., Hauswirth, W.W. and Swanson, M.S. (2003) A muscleblind knockout model for myotonic dystrophy. *Science*, **302**, 1978–1980.
42. Engel, A.G. and Franzini-Armstrong, C. (eds) (2004) *Myology*. McGraw-Hill, Inc., New York, NY.
43. Schiavon, G., Furlan, S., Marin, O. and Salvatori, S. (2002) Myotonic dystrophy protein kinase of the cardiac muscle: evaluation using an immunochemical approach. *Microsc. Res. Tech.*, **58**, 404–411.
44. Schulz, P.E., McIntosh, A.D., Kasten, M.R., Wieringa, B. and Epstein, H.F. (2003) A role for myotonic dystrophy protein kinase in synaptic plasticity. *J. Neurophysiol.*, **89**, 1177–1186.
45. Harman, D. (1981) The aging process. *Proc. Natl Acad. Sci. USA*, **78**, 7124–7128.
46. Johnson, F.B., Sinclair, D.A. and Guarente, L. (1999) Molecular biology of aging. *Cell*, **96**, 291–302.
47. Hodgson, D.M., Zingman, L.V., Kane, G.C., Perez-Terzic, C., Bienengraeber, M., Ozcan, C., Gumina, R.J., Pucar, D., O'Coclain, F., Mann, D.L., *et al.* (2003) Cellular remodeling in heart failure disrupts K_{ATP} channel-dependent stress tolerance. *EMBO J.*, **22**, 1732–1742.
48. Zingman, L.V., Hodgson, D.M., Bast, P.H., Kane, G.C., Perez-Terzic, C., Gumina, R.J., Pucar, D., Bienengraeber, M., Dzeja, P.P., Miki, T., *et al.* (2002) Kir6.2 is required for adaptation to stress. *Proc. Natl Acad. Sci. USA*, **99**, 13278–13283.
49. Nguyen, H.H., Wolfe, J.T., III, Holmes, D.R., Jr. and Edwards, W.D. (1988) Pathology of the cardiac conduction system in myotonic dystrophy: a study of 12 cases. *J. Am. Coll. Cardiol.*, **11**, 662–671.
50. Chien, K.R., Ross, J., Jr. and Hoshijima, R. (2003) Calcium and heart failure: the cycle game. *Nat. Med.*, **9**, 508–509.
51. Rüdel, R. and Lehmann-Horn, F. (1985) Membrane changes in cells from myotonia patients. *Physiol. Rev.*, **65**, 310–356.
52. Entrikin, R.K., Randall, W.R. and Wilson B.W. (1982) Myotonic electromyographic activity in complexus muscles of normal and dystrophic chicks. *Muscle Nerve*, **5**, 396–398.
53. Evans, W. (1944) The heart in myotonia atrophica. *Br. Heart J.*, **4**, 41–47.
54. O'Brien, T., Harper, P.S. and Newcombe, R.G. (1983) Blood pressure and myotonic dystrophy. *Clin. Genet.*, **23**, 422–426.
55. Pineiro, E., Fernandez-Lopez, L., Gamez, J., Marcos, R., Surralles, J. and Velazquez, A. (2003) Mutagenic stress modulates the dynamics of CTG repeat instability associated with myotonic dystrophy type 1. *Nucl. Acids Res.*, **31**, 6733–6740.
56. Tian, B., White, R.J., Xia, T., Welle, S., Turner, D.H., Mathews, M.B. and Thornton, C.A. (2000) Expanded CUG repeat RNAs form hairpins that activate the double-stranded RNA-dependent protein kinase PKR. *RNA*, **6**, 79–87.
57. Miller, J.W., Urbinati, C.R., Teng-Umnuay, P., Stenberg, M.G., Byrne, B.J., Thornton, C.A. and Swanson, M.S. (2000) Recruitment of human muscleblind proteins to (CUG)(n) expansions associated with myotonic dystrophy. *EMBO J.*, **19**, 4439–4448.
58. Gacy, M.A. and McMurray, C.T. (1998) Influence of hairpins on template reannealing at trinucleotide repeat duplexes: a model for slipped DNA. *Biochemistry*, **37**, 9426–9434.
59. Sasagawa, N., Kino, Y., Takeshita, Y., Oma, Y. and Ishiura, S. (2003) Overexpression of human myotonic dystrophy protein kinase in *Schizosaccharomyces pombe* induces an abnormal polarized and swollen cell morphology. *J. Biochem. (Tokyo)*, **134**, 537–542.
60. Engel, W.K. and Cunningham, G.G. (1963) Rapid examination of muscle tissue. An improved trichrome method for fresh-frozen biopsy sections. *Neurology*, **13**, 919–923.
61. Perez-Terzic, C., Behfar, A., Mery, A., van Deursen, J.M., Terzic, A. and Puceat, M. (2003) Structural adaptation of the nuclear pore complex in stem cell-derived cardiomyocytes. *Circ. Res.*, **92**, 444–452.
62. Perez-Terzic, C., Gacy, A.M., Bortolon, R., Dzeja, P.P., Puceat, M., Jaconi, M., Prendegast, F.G. and Terzic, A. (2001) Directed inhibition of nuclear import in cellular hypertrophy. *J. Biol. Chem.*, **276**, 20566–20571.
63. Hodgson, D.M., Behfar, A., Zingman, L.V., Kane, G.C., Perez-Terzic, C., Alekseev, A.E., Pucéat, M. and Terzic, A. (2004) Stable benefit of embryonic stem cell therapy in myocardial infarction. *Am. J. Physiol.*, **287**, H471–H479.
64. Liu, X-K., Yamada, S., Kane, G.C., Alekseev, A.E., Hodgson, D.M., O'Cochlain, F., Jahangir, A., Miki, T., Seino, S. and Terzic, A. (2004) Genetic disruption of Kir6.2, the pore-forming subunit of K_{ATP} channels, predisposes to catecholamine-induced ventricular dysrhythmia. *Diabetes*, in press.